Available online at www.sciencedirect.com
SCIENCE DIRECT®
European Journal of Mechanics B/Fluids 24 (2005) 288–295

A note on the use of one-dimensional models to describe the linear dynamics of liquid bridges

J.M. Montanero [a,*] F.J. Acero [b]

[a] *Departamento de Electrónica e Ingeniería Electromecánica, Universidad de Extremadura, 06071 Badajoz, Spain*
[b] *Departamento de Física, Universidad de Extremadura, 06071 Badajoz, Spain*

Received 6 January 2004; received in revised form 18 June 2004; accepted 7 October 2004

Available online 21 November 2004

Abstract

In this work, the capacity of the one-dimensional approximation to describe the linear dynamics of liquid bridges is studied in detail. The frequency and damping rate that characterize the first oscillation mode of a cylindrical liquid bridge are calculated from the one-dimensional models and the Navier–Stokes equations. The results are systematically compared varying Λ and C. This comparison allows one to observe the accuracy of the 1-D models and to select the most suitable one for any given values of Λ and C. This selection is expected to be correct for non-cylindrical equilibrium shapes as well. For the sake of illustration, the 1-D models are also solved numerically for non-cylindrical axisymmetric equilibrium shapes.

Keywords: Liquid bridge; Linear dynamics; One-dimensional models

1. Introduction

The theoretical analysis of liquid bridge dynamics involves great difficulties in both linear and nonlinear regimes, even for axisymmetric configurations. This is mainly due to the complex dependence of the surface tension forces on the interface deformation. For this reason, one-dimensional (1-D) models have frequently been used to study both the linear and nonlinear dynamics of liquid bridges. In the linear regime, the use of the 1-D approach allows one to obtain the characteristic equations which provide the frequencies and damping rates describing the oscillation modes of a cylindrical liquid bridge. Also, with 1-D models one can analyse the influence of the liquid bridge shape on its dynamical response with inexpensive computational resources [1,2]. Nonlinear phenomena such as breakage have been described using this kind of approximation, obtaining good agreement with the Navier–Stokes (N–S) approach in the pinch region [3].

The Lee, averaged, and parabolic models are derived by substituting a truncated Taylor series in the radial coordinate of the hydrodynamic fields into the N–S equations and boundary conditions at the interface. Also, the Cosserat model is derived by introducing the mean axial velocity into the parabolic model. A detailed description of these models and the approximations made to derive them can be found in Ref. [4]. From the analysis carried out in [4], one obtains the relative error (defined as the order of magnitude of the neglected terms divided by the order of the retained ones) of the 1-D models. The main conclusion is that the relative error is small if the dimensionless axial length scale λ is large enough [5]. The relative errors of the Lee,

* Corresponding author.
E-mail addresses: jmm@unex.es (J.M. Montanero), fjacero@unex.es (F.J. Acero).

0997-7546/$ – see front matter
doi:10.1016/j.euromechflu.2004.10.001

averaged, and parabolic models are λ^{-2}, λ^{-4}, and λ^{-4}, respectively. In the generation of the Cosserat model an inconsistency arises from neglecting some viscous terms of the same order as those retained [1,4]. For this reason, the relative error of the Cosserat model associated with the viscous terms is λ^{-2} while for the inertial terms it is λ^{-4}. These general results suggest a ranking of the 1-D models according to their accuracy. Such a ranking would, however, be applicable only for $\lambda \to \infty$. For liquid bridges, the slenderness $\Lambda \equiv L/2R_0$ (L is the distance between the supporting disks and R_0 the mean radius) is an upper bound value for λ, and its value is limited by stability requirements. A natural question is whether the aforementioned ranking also holds for finite values of λ.

In this work we shall try to answer the above question by restricting ourselves to the analysis of the small amplitude free oscillations of *cylindrical* liquid bridges. Obviously, many interesting phenomena cannot be described when nonlinear terms are completely neglected. Nevertheless, the weakly-nonlinear description of those phenomena strongly depends on a precise knowledge of linear effects [6]. Although the calculation of liquid bridge oscillations is properly an initial-value problem, here we shall not consider initial conditions. Instead, we perform a modal analysis to obtain the countable infinite set of frequencies and damping rates of the corresponding oscillation modes. The characteristic equations that provide the values of those quantities were obtained from the 1-D models mentioned above in Ref. [5]. From these equations, one finds numerically the values of the frequencies and damping rates as functions of the slenderness Λ and the capillary number $C \equiv \mu/(\rho\sigma R_0)$. Here, μ and ρ are the liquid bridge viscosity and density, respectively, while σ is the surface tension. In Ref. [5], it was shown that the aforementioned ranking in accuracy held in general: parabolic, averaged, Cosserat, and Lee models. This conclusion was drawn from a comparison with the N–S predictions for $C \leqslant 0.1$ and paramount viscosity. Although a method to solve the N–S equations for arbitrary values of C was available, the procedure would have required the calculation of the generalized eigenvalues of a matrix of high dimension (for instance, 899×899) [7].

More recently, a semi-analytical method has been proposed to calculate the frequencies and damping rates of a liquid bridge with arbitrary values of Λ and C from the N–S equations [8]. The procedure allows one to get "cheap" and accurate predictions. Here we use this method to compare the results of the 1-D models with those calculated from the N–S approach within a significant region of the Λ–C parameter plane. Finally, we present some results of integrating the 1-D models for axisymmetric liquid bridges.

2. Description of the problem

The fluid configuration considered consists of an isothermal mass of liquid of volume $\widetilde{V}$, held between two parallel coaxial disks placed a distance L apart. The radii of the disks are $R_0(1-H)$ and $R_0(1+H)$. Due to the sharpness of the disk edges, one assumes that the liquid anchors perfectly to those edges, preventing motion of the contact line. The liquid bridge is subjected to the action of a constant axial force (gravity) of magnitude g per unit mass. The liquid bridge density is ρ, the viscosity is μ, and the surface tension associated with the interface is σ. These properties are uniform and constant under the present conditions of isothermal analysis. The surrounding gas has negligible density and viscosity, so that it does not affect the dynamics of the liquid bridge. The dimensionless space and time coordinates are defined using R_0 and $t_0 \equiv (\rho R_0^3/\sigma)^{1/2}$ as the characteristic length and time, respectively. The dimensionless parameters characterizing the problem are the slenderness $\Lambda \equiv L/2R_0$, the capillary number $C \equiv \mu/(\rho\sigma R_0)$, the reduced volume $V \equiv \widetilde{V}/(\pi R_0^2 L)$, the Bond number $B \equiv \rho g R_0^2/\sigma$, and the difference parameter H between the radii of the disks.

The 1-D models considered in this paper and the approximations used to derive them were described in detail in Ref. [4]. For the sake of brevity, we will not repeat the formalism here. Let us now consider the small-amplitude free oscillations of the above fluid configuration. In order to perform a modal analysis, an exponential dependence on time $F(z,t) = \mathrm{Re}[f(z)\,\mathrm{e}^{\Omega t}]$ is introduced into the linearized models. Here F represents any (dimensionless) variable appearing in the models and z is the coordinate along the axis of the disks. The (dimensionless) eigenvalue $\Omega = \Omega_R + I\Omega_I$ characterizes the corresponding oscillation mode, Ω_R and Ω_I being the damping rate and the oscillation frequency, respectively. The most significant oscillation mode is the first for two reasons. Firstly, for common experimental conditions the magnitude of the initial amplitudes of the oscillation modes decreases rapidly as the mode index increases [2]. These amplitudes indicate the relative importance of the oscillation modes for any time if $C = 0$ (inviscid case), and for short times if $C > 0$. Secondly, if $C > 0$, the oscillation modes are damped much faster as the mode index increases. Therefore, for viscous liquid bridges the relative influence of the first oscillation mode increases with time. In addition, the accuracy of the 1-D predictions worsens as the mode index increases (λ decreases).

In this work we will focus on the calculation of the eigenvalue Ω that characterizes the first oscillation mode. For each value of C (Λ), there exists a critical value Λ_c (C_c) such that if $\Lambda < \Lambda_c$ ($C < C_c$) then Ω takes conjugate values, $\Omega = \Omega_R \pm I\Omega_I$, and if $\Lambda > \Lambda_c$ ($C > C_c$) then the values of Ω are real numbers. In the latter case and for stable configurations, one can identify two decay solutions: the *dominant* and *subdominant* motions governed by the damping factors $\Omega_R = \Omega_d$ and Ω_s ($\Omega_d > \Omega_s$),

respectively. Since $\Omega_d > \Omega_s$ the former dominates the evolution of the liquid bridge, while the latter disappears relatively quickly. Only the dominant mode will be considered.

For cylindrical liquid bridges ($V - 1 = B = H = 0$) the characteristic equations that provide the values of Ω from the 1-D models were obtained in Ref. [5]. Also, a semi-analytical method has been proposed to calculate Ω for a cylindrical liquid bridge with arbitrary values of Λ and C from the N–S equations [8]. The next section presents a comparison between these two approaches. Also, the dependence of Ω on V and B will be illustrated by the numerical integration of the 1-D models.

3. Results

3.1. Cylindrical liquid bridges

In order to illustrate the dependence of the eigenvalue Ω on the slenderness Λ, Fig. 1 shows the results for $C = 0.2$ (and $V - 1 = B = H = 0$) with the different approaches. The accuracy of the 1-D approximation increases as Λ increases. As mentioned above, there exists a critical value Λ_c beyond which Ω becomes real ($\Lambda_c \simeq 3.04$ for $C = 0.2$). This value decreases as the capillary number increases. As can be observed, all the models yield a very good estimate of the critical value Λ_c. This is true independently of the value considered for the capillary number.

The main goal of this work is to carry out an exhaustive comparison between the predictions obtained for Ω with the different approximations. To this end, let us introduce the relative errors

$$\epsilon \equiv \frac{|\Omega^{1D} - \Omega^{NS}|}{|\Omega^{NS}|}, \quad \epsilon_R \equiv \frac{|\Omega_R^{1D} - \Omega_R^{NS}|}{|\Omega_R^{NS}|}, \quad \epsilon_I \equiv \frac{|\Omega_I^{1D} - \Omega_I^{NS}|}{|\Omega_I^{NS}|}, \tag{1}$$

where the superscripts 1D and NS indicate that the solutions are obtained from a 1-D model or the N–S equations, respectively. In the present work, the eigenvalue Ω was calculated to at least 6-figure accuracy for pairs of values (Λ, C) corresponding to the nodes of a rectangular mesh of 50×50 size over $(\pi/2 < \Lambda < \pi,\ 0 < C < 1/2)$. Spline interpolation was then used to give Ω over the Λ–C plane. Fig. 2 shows the relative errors obtained from the 1-D models. As can be observed, the relative errors are quite small over the ranges of values of Λ and C considered, confirming the validity of the 1-D approximation in describing the first oscillation mode of moderately slender liquid bridges. The squared region in the right-hand graphs of Fig. 2 corresponds to values of Λ and C for which $\Omega_I^{1D} = \Omega_I^{NS} = 0$, and hence ϵ_I cannot be calculated. Note that, as was observed for Fig. 1, the values of Λ and C for which Ω_I vanishes are practically independent of the approach considered.

Table 1 lists the mean values $\langle\epsilon\rangle$, $\langle\epsilon_R\rangle$, and $\langle\epsilon_I\rangle$ for the 1-D models considered, where $\langle\cdots\rangle$ denotes the average over the region $(\pi/2 < \Lambda < \pi,\ 0 < C < 1/2)$. As can be observed, the errors obtained from the different models are similar for both the frequency and the damping rate. The predictions of the 1-D models for the frequency are more accurate than those for the damping rate. In average, the Cosserat model provides the worst prediction for the damping rate. This is probably because this quantity depends significantly on the viscosity force and, as mentioned in the Introduction, the latter is retained inconsistently in the generation of the model.

Let ϵ^{min}, ϵ_R^{min}, and ϵ_I^{min} be the minimum values of ϵ, ϵ_R, and ϵ_I, respectively, obtained using all the 1-D models for fixed values of Λ and C. Figs. 3–5 show the values of ϵ^{min}, ϵ_R^{min}, and ϵ_I^{min} (left-hand graphs), and the models used in the calculations (right-hand graphs). The grey regions correspond to the values of Λ and C for which the most accurate 1-D model cannot easily

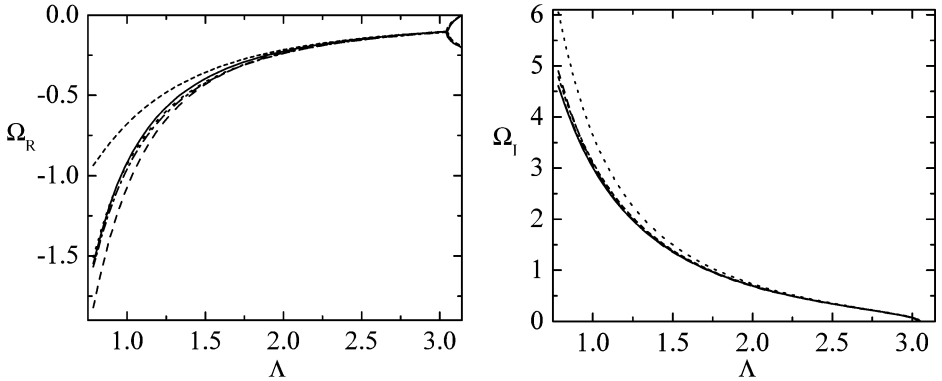

Fig. 1. Ω as a function of Λ for $C = 0.2$ ($V - 1 = B = H = 0$) obtained from the N–S (solid lines), parabolic (dashed lines), averaged (short dashed lines), Cosserat ($- \cdot -$), and Lee (dotted lines) approximations.

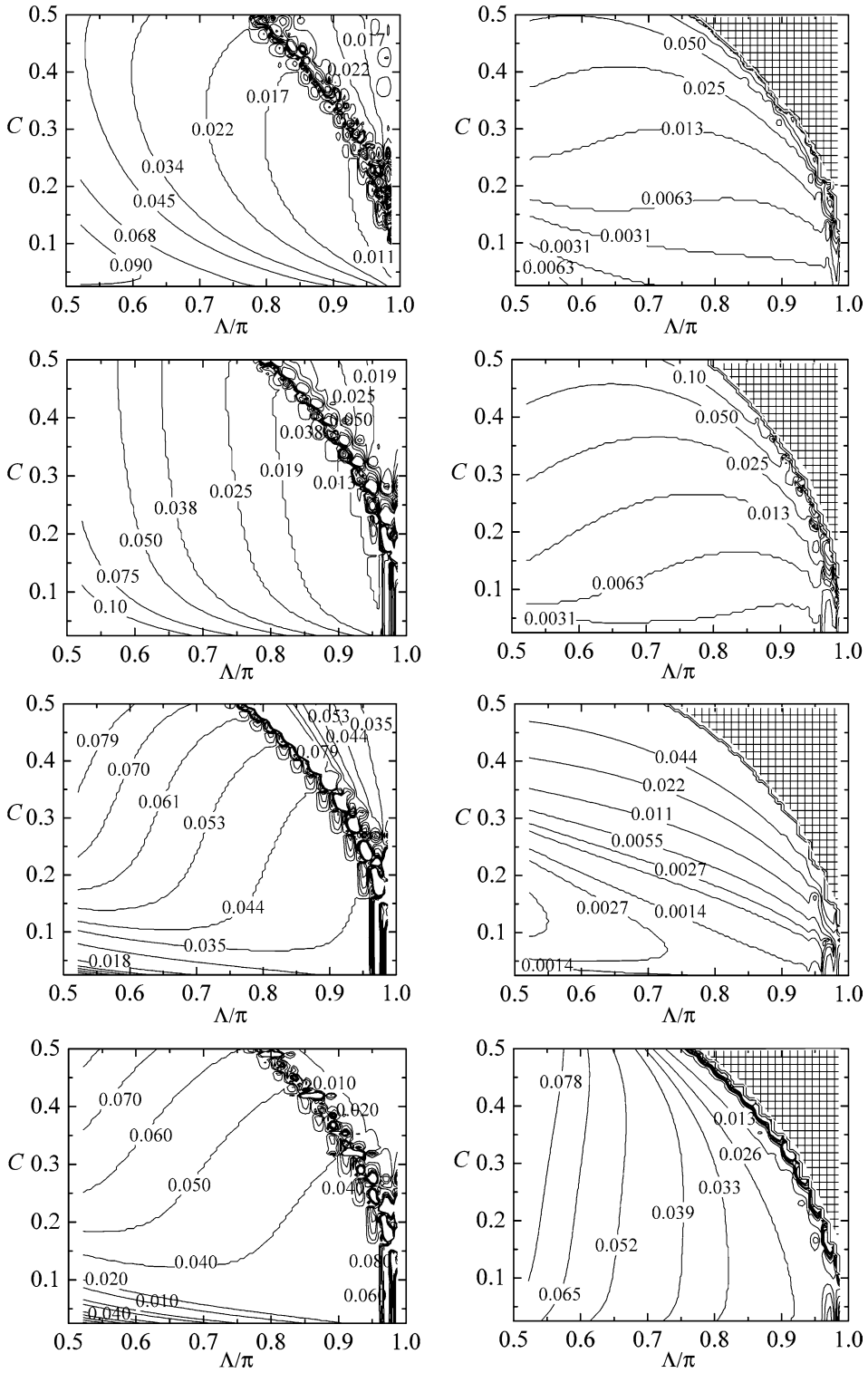

Fig. 2. Relative errors $\epsilon_R(\Lambda, C)$ (left-hand graphs) and $\epsilon_I(\Lambda, C)$ (right-hand graphs). From top to bottom the graphs correspond to the parabolic, averaged, Cosserat, and Lee models. The squared region corresponds to values of Λ and C for which $\Omega_I = 0$.

Table 1
Mean values of the relative errors for the 1-D models considered

	Lee	Cosserat	Averaged	Parabolic
$\langle\epsilon\rangle$	0.04792	0.03889	0.02725	0.02144
$\langle\epsilon_R\rangle$	0.04348	0.05245	0.03849	0.03353
$\langle\epsilon_I\rangle$	0.04063	0.03061	0.02063	0.01843

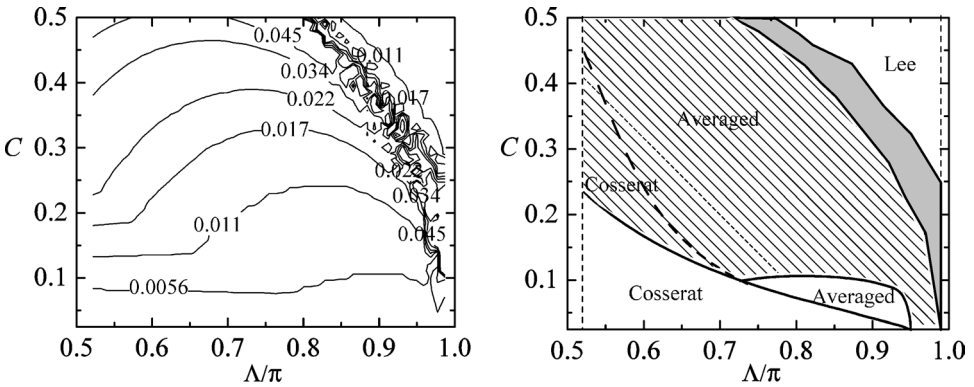

Fig. 3. Minimum relative error $\epsilon^{\min}(\Lambda, C)$ (left-hand graph) and the model used in its calculation (right-hand graph). In the right-hand graph, the ruled region indicates the values of Λ and C for which the parabolic model provides the minimum relative error. Within this region, the next model in accuracy is also indicated. The grey region corresponds to values of Λ and C for which the most accurate 1-D model can not easily be determined.

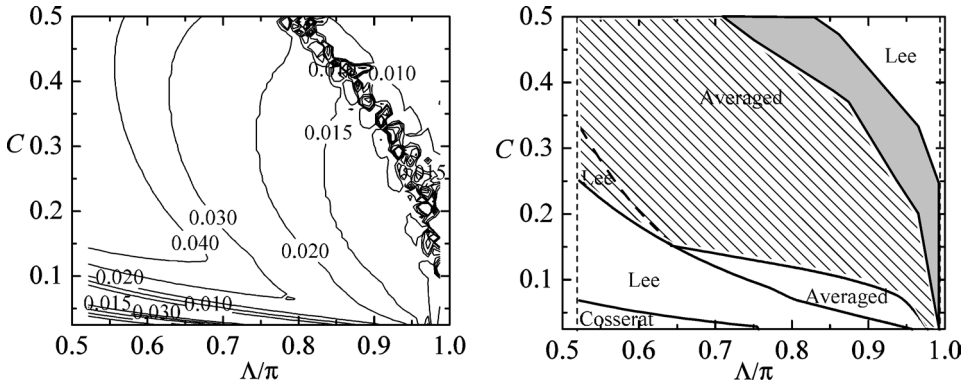

Fig. 4. Minimum relative error $\epsilon_R^{\min}(\Lambda, C)$ corresponding to the damping rate (left-hand graph) and the model used in its calculation (right-hand graph). In the right-hand graph, the ruled region indicates the values of Λ and C for which the parabolic model provides the minimum relative error. Within this region, the next model in accuracy is also indicated. The grey region corresponds to values of Λ and C for which the most accurate 1-D model cannot easily be determined.

be determined. Fig. 3 (left-hand graph) shows that the accuracy of the 1-D results increases as the slenderness increases and the capillary number decreases. From the right-hand graph of Fig. 3, one concludes that the region of the Λ–C plane where the parabolic model is the most accurate is the largest. Nevertheless, its relative accuracy (as compared with the rest of the 1-D models) does not increase as Λ increases. It must be noticed that the results obtained from the Lee model improve in some parametric range on the predictions of the rest of approximations even for large values of Λ. This suggests the use of this simple model for studying the nonlinear behaviour of viscous slender liquid bridges and jets [3]. As will be discussed below, the integration of the parabolic model for non-cylindrical shapes involves far greater difficulties than the other models. For this reason, Fig. 3 (right-hand graph) also shows the next model in accuracy within the region where the parabolic model provides the minimum relative error. Similar conclusions can be drawn from Figs. 4 and 5 for the damping rate Ω_R and the oscillation frequency Ω_I, separately. In addition, $\langle\epsilon^{\min}\rangle = 0.01808$, $\langle\epsilon_R^{\min}\rangle = 0.02384$, and $\langle\epsilon_I^{\min}\rangle = 0.01096$.

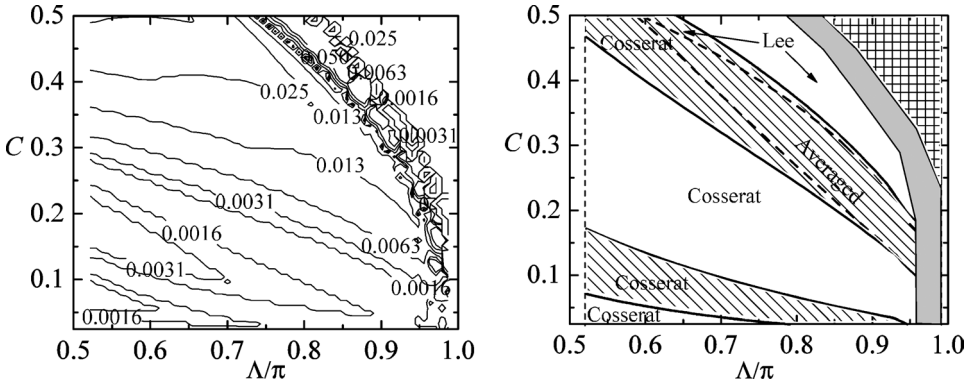

Fig. 5. Minimum relative error $\epsilon_I^{\min}(\Lambda, C)$ corresponding to the frequency (left-hand graph) and the model used in its calculation (right-hand graph). In the right-hand graph, the ruled region indicates the values of Λ and C for which the parabolic model provides the minimum relative error. Within this region, the next model in accuracy is also indicated. The grey region corresponds to values of Λ and C for which the most accurate 1-D model cannot easily be determined. The squared region corresponds to values of Λ and C for which $\Omega_I = 0$.

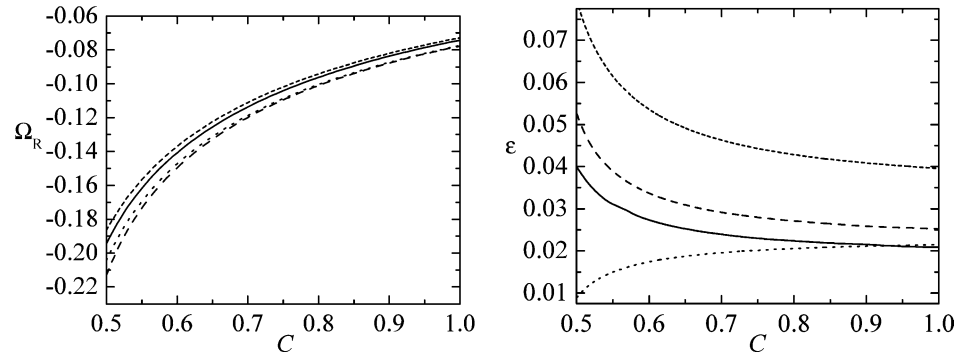

Fig. 6. Ω_R (left-hand graph) and ϵ (right-hand graph) as a function of C for $\Lambda = 2.618$ obtained from the parabolic (solid lines), averaged (dashed lines), Cosserat (short dashed lines), and Lee (dotted lines) models.

In order to show the accuracy of the 1-D approach, we have restricted ourselves to the parametrical window ($\pi/2 < \Lambda < \pi$, $0 < C < 1/2$). The interval $\pi/2 < \Lambda < \pi$ corresponds to moderately slender liquid bridges that verify the Plateau–Rayleigh stability condition $\Lambda < \pi$. A natural question is whether the global conclusions drawn from the results obtained for $0 < C < 1/2$ can be applied to different ranges of the capillary number. In the weakly viscous case, the dissipation occurs at the bulk and at the boundary layers existing on the anchors of the liquid bridge. The results showed in Ref. [5] seem to indicate that the 1-D models describes accurately the dissipation at the bulk but not that associated with the boundary layers. As a consequence, the relative error for the damping rate is expected to increase significantly as $C \to 0$. In this limit, the parabolic model behaves much better than the rest of the 1-D models [5]. This fact cannot be appreciated from Figs. 2 and 4 because the values of C chosen within this parametric region do not constitute an enough sample.

Beyond the upper limit $C = 1/2$ and for the range of slenderness considered in our analysis, the distinction between the oscillation modes is not clear [2,8], and the liquid bridge dynamics may not be represented adequately by only the first oscillation mode. For this reason, a comparison between the predictions obtained for the latter from the different approaches is less significant. Fig. 6 shows the damping rate Ω_R ($\Omega_I = 0$) and the relative error $\epsilon = \epsilon_R$ for $\Lambda = 2.618$ and $1/2 < C < 1$. To be sure that the oscillation mode considered is the dominant one, i.e., the mode with the smaller value of $|\Omega_R|$, a graphical analysis of the characteristic equations has been performed for each value of C. The relative errors are similar to those obtained within the interval $0 < C < 1/2$. It must be pointed that two kinds of oscillation modes, called capillary and hydrodynamic respectively, are almost always clearly identified but become melted for $1/2 < C < 1$ [8]. The interface deformation plays an essential role in the capillary modes but is unimportant in the hydrodynamic ones. The parabolic model predicts the appearance of the first hydrodynamic mode but very inaccurately [5,8]. Nevertheless, and at least for the slenderness considered in Fig. 6, the first capillary oscillation mode is the dominant mode not only for $0 < C < 1/2$ but also for $1/2 < C < 1$. It is worthwhile mentioning that because different oscillation modes coalesce for $1/2 < C < 1$, the numerical algorithms used to find the roots Ω of the characteristic equations are increasingly costly beyond $C \simeq 1/2$.

3.2. Non-cylindrical liquid bridges

There are two possible causes of the deformation of the equilibrium liquid bridge contour (between supporting disks of equal radius): (i) gravity and (ii) the excess or defect of the volume of liquid relative to the cylinder. The former is always present, excepting in space and in-flight experiments, although its effect can be reduced by the use of microzones. The latter is frequently related to the evaporation of liquid during the experiment. Therefore, experimental conditions that allow one to study the evolution of a *cylindrical* liquid bridge are hard to achieve. The main advantage of using the 1-D approach is perhaps the possibility of obtaining theoretical predictions for non-cylindrical equilibrium shapes while maintaining a certain simplicity. For the sake of illustration, we shall determine the frequency and damping rate of the first oscillation mode for different equilibrium contours from the 1-D models considered.

The numerical procedure is the same for the Lee, averaged, and Cosserat models. Here we only briefly describe the method. The details can be found in Ref. [2]. The problem can be formulated in terms of a function $S(z)$ which characterizes the interface position, and the axial momentum $Q(z)$. These functions are to be determined from the continuity and momentum equations together with the corresponding boundary conditions. In the first order, S is eliminated from the formulation by considering the continuity equation. Then the momentum equation becomes a fourth-order differential equation for Q. This equation and the boundary conditions constitute a two-point boundary value problem which can be solved by transforming it to an initial-value problem. The eigenvalues are those for which the Jacobian of the transformation vanishes. The dependence of Ω on the parameters of the system was analysed in Ref. [2] using the Cosserat model. The scheme used to integrate the parabolic model is basically the same excepting that in this case one has to deal with two coupled fourth-order differential equations for the two functions involved (the linear and quadratic contributions to the axial momentum), so that the equivalent differential order of the problem is eight. The eigenvalues characterizing the oscillation modes are also identified by setting to zero the Jacobian of the corresponding transformation. Due to the higher order of the Jacobian, the search for this root is a difficult task.

The numerical procedures described above were tested by comparing the results with those obtained for cylindrical liquid bridges from the characteristic equations. The numerical solutions were found to have at least 6-figure accuracy. Figs. 7 and 8 show, for illustration, the dependence of Ω on V and B, respectively, as obtained from the 1-D models with the rest of the

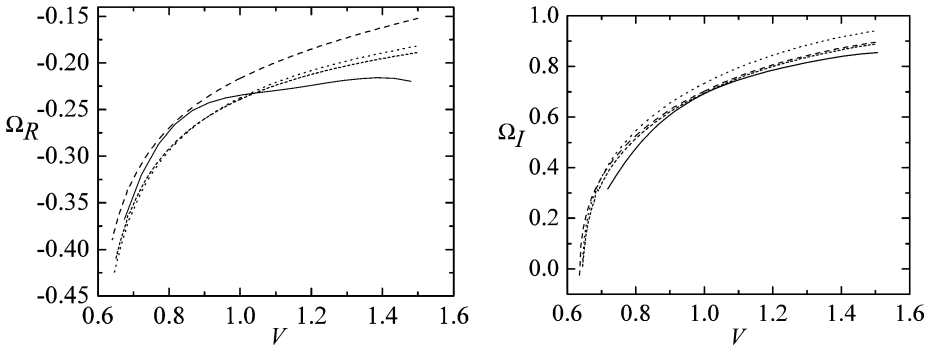

Fig. 7. Ω as a function of V for $\Lambda = 2$, $C = 0.2$, and $B = H = 0$ obtained from the parabolic (solid lines), averaged (dashed lines), Cosserat (short dashed lines), and Lee (dotted lines) models.

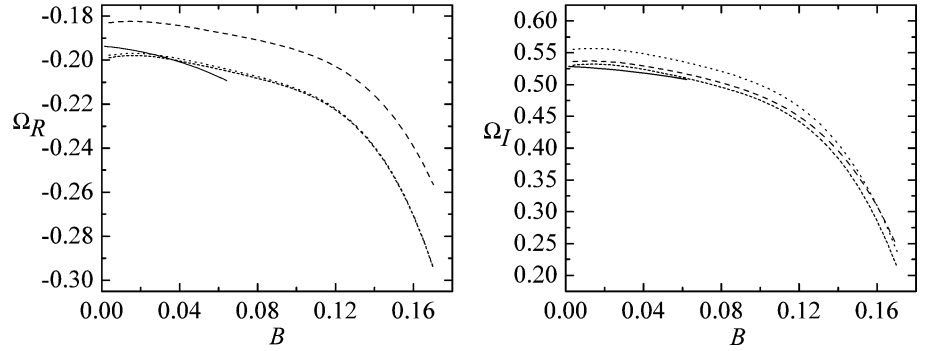

Fig. 8. Ω as a function of B for $\Lambda = 2.2$, $C = 0.2$, and $V - 1 = H = 0$ obtained from the parabolic (solid lines), averaged (dashed lines), Cosserat (short dashed lines), and Lee (dotted lines) models.

parameters fixed. The observed trends were similar for all the models considered. Due to the difficulties in determining Ω with the parabolic model for large values of B, only results for $B \leqslant 0.06$ are plotted in Fig. 8. The results given in Ref. [7] for $B \neq 0$ were restricted to $\Lambda \leqslant \pi/2$, and hence no significant comparison with the present predictions for slender liquid bridges is possible. The comparison between the N–S and Cosserat approaches for non-cylindrical inviscid liquid bridges indicates a good agreement [9].

4. Concluding remarks

In sum, this paper has discussed the use of 1-D models to analyse the linear dynamics of liquid bridges. The 1-D approach has often been used to describe the dynamics of jets and slender liquid bridges because it is known to provide valuable results both qualitatively and quantitatively if the length scale λ of the system is sufficiently large. The relative simplicity of the linear dynamics of cylindrical liquid bridges allows one to assess the accuracy of the models for finite values of λ by comparison with "exact" results. The values given in Table 1 demonstrate that this approach provides an accurate description of the first oscillation mode in a significant region of the Λ–C plane. Figs. 3–5 show the results calculated from the most accurate model for given values of Λ and C.

The use of the 1-D approach allows major simplifications when interface deformations of finite amplitude are present. This is not only the case in such nonlinear phenomena as breakage, but also in the linear evolution of liquid bridges with non-cylindrical equilibrium shapes. For practical purposes one must apply accuracy and simplicity criteria in selecting the appropriate model. The averaged and the Cosserat models verify both criteria over a wide range of values of Λ and C. The integration of the parabolic model involves far greater difficulties than the others, but it does not significantly improve the results for $\Lambda < \pi$ (the Plateau–Rayleigh stability limit). In spite of its simplicity, the Lee model also provides valuable results, and thus it could be a good candidate to describe more complex phenomena that include nonlinear effects.

It is known that matching experimental and calculated equilibrium shapes for various Bond numbers leads to accurate estimates of the surface tension when the liquid bridges are slender [10]. Using the same fluid configuration, the viscosity value (capillary number) can be inferred by fitting experimental data of the damping rate with the 1-D predictions. The damping rate of the first oscillation mode is very approximately proportional to the capillary number within the interval $0 \leqslant C \leqslant C_c(\Lambda)$ [2,5]. Therefore, the relative error obtained for C within that interval is similar to ϵ_R. For viscous liquid bridges, the damping rate can be measured with accuracy, the 1-D approximation provides good predictions for this quantity, and hence this method is expected to provide accurate values of the liquid bridge viscosity. Besides, given that the calculations involved are relatively simple and can be easily automated, the efficiency of the procedure is likely to be acceptable.

Acknowledgement

Partial support from the MCYT (Spain) through Grant No. ESP2003-02859 is acknowledged.

References

[1] J.M. Perales, J. Meseguer, Theoretical and experimental study of the vibration of axisymmetric viscous liquid bridges, Phys. Fluids A 4 (1992) 1110–1130.
[2] J.M. Montanero, Linear dynamics of axisymmetric liquid bridges, Eur. J. Mech. B Fluids 22 (2003) 169–178.
[3] J. Eggers, Nonlinear dynamics and breakup of free-surface flows, Rev. Mod. Phys. 69 (1997) 865–929.
[4] F.J. García, A. Castellanos, One-dimensional models for slender axisymmetric viscous liquid jets, Phys. Fluids 6 (1994) 2676–2689.
[5] F.J. García, A. Castellanos, One-dimensional models for slender axisymmetric viscous liquid bridges, Phys. Fluids 8 (1996) 2837–2846.
[6] J.A. Nicolás, J.M. Vega, Weakly nonlinear oscillations of axisymmetric liquid bridges, J. Fluid Mech. 328 (1996) 95–128.
[7] J. Tsamopoulos, T. Chen, A. Borkar, Viscous oscillations of capillary bridges, J. Fluid Mech. 235 (1992) 579–609.
[8] J.A. Nicolás, J.M. Vega, Linear oscillations of axisymmetric viscous liquid bridges, Z. Angew. Math. Phys. 51 (2000) 701–731.
[9] J.M. Montanero, Theoretical analysis of the vibration of axisymmetric liquid bridges of arbitrary shape, Theoret. Comput. Fluid Dynamics 16 (2003) 171–186.
[10] M.G. Cabezas, J.M. Montanero, J. Acero, M.A. Jaramillo, J.A. Fernández, Detection of the liquid bridge contour and its applications, Meas. Sci. Technol. 13 (2002) 829–835.